UNCLASSIFIED

AD 274 219

Reproduced
by the

ARMED SERVICES TECHNICAL INFORMATION AGENCY
ARLINGTON HALL STATION
ARLINGTON 12, VIRGINIA

UNCLASSIFIED

FEASIBILITY OF A DIFFUSER CENTERBODY INJECTOR FOR THE 16-FOOT SUPERSONIC TUNNEL OF THE PROPULSION WIND TUNNEL FACILITY

By

E. H. Sloan, Jr. and M. W. Davis

Propulsion Wind Tunnel Facility

ARO, Inc.

TECHNICAL DOCUMENTARY REPORT NO. AEDC-TDR-62-75

April 1962

ARNOLD ENGINEERING DEVELOPMENT CENTER
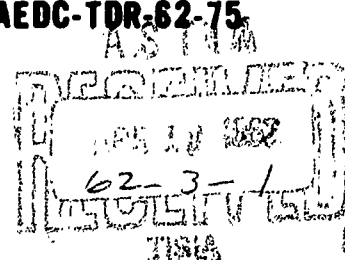
AIR FORCE SYSTEMS COMMAND

UNITED STATES AIR FORCE

FEASIBILITY OF A DIFFUSER CENTERBODY INJECTOR FOR THE 16-FOOT SUPERSONIC TUNNEL OF THE PROPULSION WIND TUNNEL FACILITY

By

E. H. Sloan, Jr. and M. W. Davis

Propulsion Wind Tunnel Facility

ARO, Inc.,

a subsidiary of Sverdrup and Parcel, Inc.

April 1962

ARO Project No. 230956

AF - AEDC
Arnold AFB Tenn

ABSTRACT

A centerbody injector for reducing the pressure ratio required to operate the 16-Ft Supersonic Tunnel of the Propulsion Wind Tunnel Facility has been investigated analytically, and several configurations have been tested in the Supersonic Model Tunnel.

The injectors were fitted to the existing scavenging scoop centerbody so that secondary air routed through the scavenge ducting is introduced just downstream of the minimum area of the variable geometry diffuser.

The results obtained from the best tip injector system, with respect to the running pressure ratio at M = 5. 0, ranged from a 36-percent improvement with the injector air off to a 52-percent improvement with the maximum tolerable air injection over the data from the closed aerodynamic scoop tip.

CONTENTS

TABLES

ILLUSTRATIONS

Figure

NOMENCLATURE

A	Cross-sectional area of a stream tube or channel, $in.^2$
c_p	Specific heat at constant pressure, $ft^2/sec^2 \, °R$
D	A Mach number function ($\gamma = 7/5$), $D = \dfrac{M}{(1 + 0.2M^2)^3}$
G	A Mach number function ($\gamma = 7/5$), $G = \dfrac{1 + 1.4M^2}{(1 + 0.2M^2)^{7/2}}$
h	Tunnel height, in.
ΔL_1	Length of the first leaf in the variable geometry diffuser, in.
M	Mach number
m	Mass flow, slugs/sec
$\overset{\circ}{m}$	Static pressure mass flow function, $\overset{\circ}{m} = \dfrac{W\sqrt{T_t}}{pA}$, $\sqrt{°R}/sec$
N	A Mach number function ($\gamma = 7/5$), $N = \dfrac{D}{G} = \dfrac{M(1 + 0.2M^2)^{1/2}}{1 + 1.4M^2}$
p	Static pressure, lb/ft^2 (psf)
p_t	Stagnation pressure, lb/ft^2 (psf)
r	Injector mass flow ratio, $r = m_j/m_n{}^*$
T	Static temperature, °R unless indicated
T_t	Stagnation temperature, °R unless indicated
W	Weight flow, lb/sec
γ	Ratio of specific heats
δ_e	Effective two-dimensional wedge angle, deg
η_d	Isentropic subsonic diffuser efficiency
θ_e	Effective shock angle from an effective two-dimensional wedge, deg
θ_j	Injector stagnation temperature ratio, $\theta_j = T_{t_j}/T_{t_o}$
λ	Tunnel pressure ratio, $\lambda = p_{t_o}/p_{t_s}$
ρ	Airstream static density, $slugs/ft^3$
ρ_t	Airstream stagnation density, $slugs/ft^3$

vii

SUPERSCRIPT

$*$ Sonic or critical conditions

SUBSCRIPTS

e   Effective

j   Injector conditions

n   Nozzle conditions

o   Stilling chamber conditions

r   Pertaining to conditions at minimum-running pressure ratio

s   Pertaining to conditions at the minimum-starting pressure ratio

1   Test section conditions

2   Diffuser minimum area conditions

3   Conditions ahead of tunnel terminal shock (see sketch on page 20)

4   Conditions behind tunnel terminal shock (see sketch on page 20)

5   Diffuser exit conditions (see Fig. 1 and sketch on page 20)

1.0 INTRODUCTION

The 16-Ft Supersonic Tunnel of the Propulsion Wind Tunnel Facility (PWT-16S) has a test section size of 16 by 16 by 40 ft and is a continuous-flow, closed-circuit wind tunnel capable of operating at stagnation pressure levels up to approximately one atmosphere. The Mach number is controlled by a flexible nozzle designed to operate between the Mach numbers of 1.5 and 5.0. The compressor for this wind tunnel consists of four axial-flow compressors (cylinders) in tandem with the option of selecting 4, 8, 12, or 18 stages of compression by use of remote couplings and iris valves. The four-cylinder configuration is capable of producing a maximum pressure ratio of approximately eight.

To make it possible to operate this wind tunnel in the Mach number range between approximately 3.25 to 4.0 with pressure ratios below eight, a variable geometry diffuser has been provided. The operational philosophy is that after flow is established in the low Mach number range (that is, less than 3.25), the nozzle and diffuser are varied in small increments to reach the high test section Mach numbers. The tunnel also includes a duct to remove combustion products produced by a propulsion test unit. This scavenging scoop forms a centerbody through the variable geometry diffuser.

Since the open scavenging scoop is not necessary for aerodynamic testing, a series of model tunnel investigations were undertaken to develop a closed-off scoop tip configuration. The results of these model tests indicated that the optimum running pressure ratio ranges from about 15 percent below the normal shock pressure ratio at M = 1.8 to M = 3.5 to about 10 percent above the normal shock curve at M = 5.0.

Because the diffuser and compressor performance of the full-scale tunnel limits the empty tunnel top Mach number to approximately 4.0, alternate methods of lowering the running pressure ratio at high Mach numbers were studied. A preliminary feasibility study of a relatively inexpensive diffuser injector was made, and a series of model studies were undertaken.

The performance gain produced by an auxiliary diffuser injector on a conventional normal shock diffuser is well known (Refs. 1, 2, and 3). More recent diffuser injector work by NACA (Ref. 4) indicates additional gains were possible when the injected air was introduced at the minimum area of a variable geometry diffuser. This method resulted in a reduction of the optimum running pressure ratio by a factor of

Manuscript released by authors March 1962.

1

approximately eight at M_1 = 5.0. This outstanding performance required injector mass flows on the order of six times the test section mass flow for the Mach number 5 condition. Ordinarily, for a compressor matched to the tunnel mass flows with a reasonably good variable geometry diffuser performance, injector mass flow ratios this large would incur undue power penalties. However, matching the PWT-16S compressor to the tunnel requires bypassing increasing amounts of air for nozzle contours above approximately 3.4 to keep the compressor within its inlet volume flow capacity. For this reason, reasonably large auxiliary mass flows are available to operate an injector for Mach numbers above 3.4.

Two methods are apparent for applying the diffuser-throat injector principle of Ref. 4 to the PWT-16S: (1) modification of the variable geometry diffuser to have sidewall injector nozzles similar in design to the Ref. 4 system, and (2) modification of the closed-off scoop tip into a centerbody annular exit type of injector nozzle, utilizing the scavenging ducting as part of the induction system. The first method would probably produce the better result for the same injector mass flow ratio since the more troublesome sidewall boundary layer would be energized. However, the large additional cost of an induction plenum, sidewall injector nozzles, and new diffuser backup structure, makes the centerbody scheme more attractive.

To estimate the performance of a centerbody injector scheme and define the variables of interest, a theoretical analysis was undertaken. Preliminary results from this analysis were used to define the initial injector geometry. A model of the injector was fabricated, and tests were conducted intermittently in the Supersonic Model Tunnel (SMT) between April 1959 and October 1960. During the test period the original design was modified to improve the performance, and an additional tip was made to check out a limited variation of the concept.

2.0 THEORETICAL CONSIDERATIONS

The approach used in determining the theoretical performance of the injector system depends upon the evaluation of three separate but interrelated phases of the overall diffusion process. The three divisions to be considered are: (1) the supersonic diffuser, (2) the injector (or mixing) region, and (3) the subsonic diffuser.

The supersonic diffusion process for this type of injector configuration is complicated by the presence of the centerbody in the supersonic diffuser. Therefore, the inviscid two-dimensional model of the

supersonic diffuser that is sometimes employed to estimate the diffuser performance should not be directly applied in this case. Instead, a hypothetical supersonic diffuser is considered which has the same length and net area change as the actual diffuser. A combination of one and two-dimensional methods is then used to find the Mach number and the ratio of the local static pressure to the tunnel stagnation pressure at the supersonic diffuser minimum area.

The equations that result from this approach for determining the Mach number and static-to-stagnation pressure ratio are (see sketch on page 20 for notation):

$$M_2 = \left[-2.50 + \sqrt{6.250 + 5.9214 \ \overset{\circ}{m}_2{}^2}\right]^{1/2}$$

where

$$\overset{\circ}{m}_2 = \frac{0.53177}{\left(\frac{P_2}{P_{t_1}}\right)\left(\frac{A_1}{A_n{}^*}\right)\left(\frac{A_2}{A_1}\right)}$$

and

$$\frac{P_2}{P_{t_1}} = \frac{7M_1{}^2 \ \sin^2 \theta_e - 1}{6}\left[\frac{5}{M_1{}^2 + 5}\right]^{7/2}$$

Further discussion of these equations is given in Appendix I.

The main mechanisms that enable a diffuser injector to improve the overall diffuser recovery occur in the mixing region and are reported in Ref. 4 as:

1. The introduction of a higher stagnation pressure ahead of the normal shock system in the constant-area portion of the diffuser (shock duct) increases the stagnation pressure level of the mixed stream. Therefore, after traversing the shock system, the stream stagnation pressure is higher than it would normally be without injected flow.

2. The high energy stream from the injector energizes the boundary layer, which lessens the interaction losses from the shock system.

3. At slightly higher static pressure than the primary stream, an expanding injector stream produces additional oblique shock deceleration to the main flow.

The last two mechanisms are not amenable to a simple theoretical treatment, but the first mechanism can be approximated by a relatively simple one-dimensional mixing process with constant area for an inviscid medium. The solution of the pressure recovery provided by

3

such a mixing process can be found by the use of the Mach number functions defined and tabulated in Ref. 5 and the equation,

$$\frac{P_{t_3}}{P_{t_1}} = \frac{P_{t_2}}{P_{t_1}} \left[\frac{\left(\frac{A_2}{A_1}\right)\left(\frac{A_1}{A_n{}^*}\right)}{\left(\frac{A_2}{A_1}\right)\left(\frac{A_1}{A_n{}^*}\right) + \frac{A_j}{A_n{}^*}} \right] \frac{G_2}{G_3} + \frac{P_{tj}}{P_{t_1}} \left[\frac{\frac{A_j}{A_n{}^*}}{\left(\frac{A_2}{A_1}\right)\left(\frac{A_1}{A_n{}^*}\right) + \frac{A_j}{A_n{}^*}} \right] \frac{G_j}{G_3}$$

where

$$G_3 = f(M_3)$$

and

$$M_3 = f(N_3)$$

and

$$N_3 = \frac{(1 + r)^{1/2}\,(1 + r\,\theta_j)^{1/2}}{\dfrac{1}{N_2} + \dfrac{r\,\theta_j{}^{1/2}}{N_j}}$$

and from Ref. 6

$$\frac{P_{t_2}}{P_{t_1}} = \frac{P_2}{P_{t_1}}\left[1 + 0.2M_2{}^2\right]^{7/2}$$

Derivation of the preceding equations are given in Appendix I.

To complete the performance estimate through the mixing region, the pressure recovery after the mixing process is assumed to be equal to the normal shock recovery at the mixed Mach number.

Consequently,

$$\frac{P_{t_4}}{P_{t_3}} = \left[\frac{6M_3{}^2}{M_3{}^2 + 5}\right]^{7/2}\left[\frac{6}{7M_3{}^2 - 1}\right]^{5/2} \tag{1}$$

The subsonic diffusion process may be represented by the concept of an isentropic diffuser efficiency as follows (from Ref. 7):

$$\frac{P_{t_5}}{P_{t_4}} = \left[\frac{2 + 0.4M_4{}^2\,\eta_d}{2 + 0.4M_4{}^2}\right]^{7/2} \tag{2}$$

where M_4 is the Mach number behind a normal shock with entrance Mach number M_3, which may be expressed from Ref. 6:

$$M_4 = \left[\frac{M_3{}^2 + 5}{7M_3{}^2 - 1}\right]^{1/2} \tag{3}$$

4

Now the overall pressure ratio is found as follows:

$$\frac{1}{\lambda_r} = \frac{P_{t_5}}{P_{t_1}} = \left(\frac{P_{t_5}}{P_{t_4}}\right)\left(\frac{P_{t_4}}{P_{t_3}}\right)\left(\frac{P_{t_3}}{P_{t_1}}\right) \tag{4}$$

All that is needed now to predict the overall injector diffuser performance for a particular injector configuration is the geometry of the diffuser-injector combination and the injector and tunnel stagnation conditions. Although the theory cannot establish practical operating limits for the various geometric and flow parameters, it should provide a valid indication of the effect of these parameters and determine which are most important.

3.0 MODEL TUNNEL TESTS

3.1 APPARATUS

The Supersonic Model Tunnel in which the model injector tests were performed is a 1/16-scale model of the 16-Ft Supersonic Tunnel flow converter section including the variable geometry diffuser and scavenging system.

At the time of the injector tests only two sets of fixed nozzle blocks were available, Mach number 2.0 and Mach number 3.5. These nozzle blocks were used to obtain all of the Mach numbers for the test: namely, M_1 = 2.2, 3.15, 3.5, 3.9, 4.0, and 5.0. Mach number 2.2 was generated by tilting the M_1 = 2.0 blocks. Mach numbers 3.15, 3.9, and 4.0 were obtained by tilting the M_1 = 3.5 blocks, and M_1 = 5.0 was obtained by making a plaster-of-Paris overlay on the M_1 = 3.5 blocks. In general, the flow quality was poor except for the design Mach number of the blocks; however, it was considered adequate for the purpose of the test.

The general arrangement of the model tunnel diffuser is shown in Fig. 1. The model tunnel diffuser consists of fixed sidewalls one foot apart and movable top and bottom walls. Each movable wall is made up of five hinged sections. These sections are positioned by screwjacks that are manually actuated from outside the tunnel. The first four sections are fixed in length with the fifth section telescoping to compensate for the longitudinal change in length as the walls are moved. The opening at each frame station is indicated by calibrated counters geared to the jacking mechanism. A pair of wedge-shaped inserts were available that could be attached to the rear half of the test section top and bottom walls to simulate wall convergence in the

5

rear half of the test section, a feature of the second cart in the 16-Ft Tunnel. This feature almost doubles the supersonic diffuser length which should be beneficial at the higher Mach numbers.

The first test runs with an injector were made with the scavenging scoop line open to the atmosphere and ambient air used for the injector. This arrangement made it difficult to determine the maximum p_{t_j}/p_{t_o} ratio for stable flow conditions. Therefore, between testing of the first and second injector models, a bypass line connecting the tunnel supply line with the scoop ducting was installed. This bypass line made it possible to supply the maximum plant pressure (about 40 psia) to the injector.

The general arrangement of the closed aerodynamic scoop tip that is used for performance comparison purposes is shown in Fig. 2.

Details of the injector tips are presented in Figs. 3, 4, and 5. Some of the factors that affected or were considered in the design of the injectors are:

1. The injector Mach number should be approximately 2.6, or higher, so that the static pressure at the injection station will be about the same magnitude as the mainstream static pressure.

2. The maximum skirt diameter should be approximately 9.6 in. to allow starts at or above a nozzle setting of approximately 2.5.

3. The injector exit should be a reasonable distance downstream of the variable geometry diffuser minimum area to insure stabilized flow in the mainstream.

4. The injector tip should start at tunnel station 31.9 in. so that cart roll-out, a feature of the 16-Ft Tunnel, may be accomplished for any test article that will clear the retracted diffuser.

5. The constant-area mixing duct downstream of the injector exit should be sufficiently long to insure near complete mixing of the main and injector streams.

6. The injector tip should be easily removed to allow setup of the conventional propulsion scoop tip. This implies that a joint upstream of the support strut should be the disconnect point if possible.

6

Injector A (Fig. 3) meets these requirements reasonably well; however, the results of the initial test runs indicated that the performance was not as good as is theoretically possible. To improve Injector A performance a longer foretip of different design was fitted to the existing injector nozzle section. This was called Injector B (Fig. 4). An ogive foretip for Injector B would have been desirable, but the fabrication of a full-scale ogive would have been difficult and expensive. Therefore, a series of conic frustum sections that result in a near ogive shape were used. The Injector B tip violates Item 4 design criteria, but it is believed that objections to the use of such a tip could be overcome by providing adequate handling equipment for tip removal. The improved performance provided by Injector B led to the design of Injector C which, it was felt, should further improve the injector performance because of the reduced diameter at the injector section. This skirt size reduction was made possible by inverting the injector nozzle contour and inclining the injector flow 15 deg to the tunnel centerline (see Fig. 5).

The injector nozzle contour for all injectors was designed using the method of Ref. 8 by assuming the annular nozzle to be two-dimensional in nature. The results of this computation method are tabulated in Table 1. By examination of Table 1 it is seen that the two-dimensional flow turning angle is 39. 12 deg, the value for an exit Mach number of 2. 5, while the inviscid area ratio for the three-dimensional geometry specified a Mach number of 2. 71. Static pressure measurements, however, showed that the resulting Mach number obtained was approximately 2. 6.

The injector tips were instrumented for pressure measurements in the following manner: (1) a manifold ring of four total pressure probes, one in each quadrant, in the annular air passage ahead of the nozzle throat, (2) a static pressure orifice in each quadrant of the injector nozzle exit plane, and (3) a static orifice in each quadrant on the outside of the injector skirt, open to the tunnel airstream just ahead of the nozzle exit. Two of the latter orifices were approximately in the horizontal plane and two in the vertical plane. This instrumentation is shown in Figs. 3, 4, and 5 for the various injectors.

The injector supply line is equipped with an orifice plate that was used for determining the injector mass flow.

The tunnel pressure instrumentation consisted of (1) a manifold ring of four total pressure probes in the settling chamber, (2) wall static orifices throughout the tunnel nozzle and diffuser on the wall centerline, (3) four total pressure probes equally spaced around the

annular passage downstream of the variable geometry diffuser (see Fig. 1), and (4) the same as (3) except that one of the total pressure probes was replaced with a rake and four static orifices were added.

The measured pressures were displayed on a mercury manometer board and recorded photographically. The tunnel stagnation pressure, the diffuser-exit total and static pressures, the injector-skirt static pressure in both the horizontal and vertical planes, and a wall static pressure near the diffuser entrance were also recorded by an oscillograph.

3.2 TEST PROCEDURE

The parameter used to evaluate the injector-diffuser performance is the overall minimum pressure ratio. The object of the experiment was to define the minimum pressure ratio for each configuration over the available Mach number range for an empty tunnel with solid test section walls. This was performed by establishing the tunnel and injector flow conditions, setting the variable geometry diffuser to the desired contour, and then increasing the tunnel exhaust pressure continuously, while maintaining a constant p_{t_o}, until the tunnel flow broke down. Oscillograph records were obtained during the time the exhaust pressure was varied. Additionally, a photograph of the manometer board was made before the exhaust pressure was changed and, as far as it was possible, at the time flow broke down. The minimum diffuser area was obtained while holding other test conditions the same. The variable geometry diffuser height at Frame 2 was closed in quarter-inch increments until the diffuser area ratio, A_2/A_1, reached the point that caused flow breakdown because of insufficient second throat area. The oscillograph records were reduced to obtain the minimum tunnel pressure ratio, λ_r, at the point where flow broke down; this point was determined from a discontinuity in the trace produced by the static pressure near the diffuser entrance.

The Reynolds number based on the height of the test section and a stagnation pressure of 20 pounds per square inch absolute and a stagnation temperature of 100°F varied from 4.45 x 10^6 to 1.07 x 10^6 over the Mach number range from 2.2 to 5.0. The actual Reynolds number varied around these values because of the range of stagnation pressures used to set the p_{t_j}/p_{t_o} ratio and variations in the stagnation temperature. For Injector A, which used ambient atmospheric air, the p_{t_j}/p_{t_o} ratio was controlled by regulating p_{t_o}; for Injectors B and C, using the bypass line, the p_{t_j}/p_{t_o} ratio was controlled by varying p_{t_j}. Injector C required

tunnel stagnation pressures as high as 40 psia at M_1 = 5.0 for satisfactory tunnel operation.

The tunnel stagnation temperature varied from approximately 85°F to 160°F. At times the temperature was low enought at M = 5.0 for liquifaction to occur; however, no adverse effects were noted.

Two methods were used to determine the diffuser exit pressure during the tests. For Injector A, the four total pressure probes, labeled p_{t_5} in Fig. 1, were manifolded together, and the resulting pressure was considered as the diffuser-exit total pressure. However, flow fluctuations, possibly caused by separation and re-attachment, resulted in pressure oscillations that made reading difficult. A rake was installed in the place of one of the total pressure probes and confirmed the hypothesis that the velocity profile across the channel changed radically as the exhaust pressure varied. Static pressure orifices were then added for the Injector B and C tests, and the total pressure was calculated by the continuity area average method (Ref. 9) using the average static pressure, the area at the measuring station, and the combined mass flow through the tunnel and the injector. In general, pressure ratios obtained by the continuity average method were slightly higher (more conservative) than those obtained from the directly measured exit total pressure.

The diffuser configurations used for the test all had the minimum area at the Frame 2 station, as dictated by the design, but four different basic diffuser contours were used during the test.

The difference between the contours is illustrated in Fig. 6. Contour number one had a two-degree total effective divergence between Frames 2 and 4. A straight line fairing was used from Frame 4 to the diffuser exit unless the angle formed between the movable section 4 and the centerline would exceed four degrees. A four-degree limit was placed on this angle to prevent flow separation. For contour number two, Frames 3, 4, and 5 were opened as far as the jack travel would allow. Contour number three is similar to contour number two with the opening at Frames 3, 4, and 5 held at 15 in. instead of the maximum opening. For contour number four, Frames 3, 4, and 5 were set in a group according to the table for contour number one but were positioned independently of Frame 2.

9

4.0 RESULTS

Two typical plots of the minimum-running pressure ratio versus the diffuser contraction ratio are presented in Fig. 7. Injector B appears to be slightly more sensitive to the diffuser contraction ratio (Fig. 7a) than Injector C (Fig. 7b); however, the general insensitivity to area ratio shown in these figures is characteristic of the test results. It was necessary to vary the area ratio to find the optimum-area pressure ratio and minimum area ratio for a given injector-diffuser configuration. However, the minimum area ratio at which flow could be maintained does not necessarily result in the lowest pressure ratio as might be expected. Therefore, the area ratio may be considered as somewhat the minor parameter, and the discussion hereafter will be conducted in terms of the tunnel pressure ratio and the injector-to-tunnel stagnation pressure ratio. It is also realized that one of the most important parameters associated with injectors is the mass flow ratio. However, if the injector geometry is fixed and the ratio of the stagnation temperatures remains constant, the mass flow ratio is a linear function of the stagnation pressure ratio for supercritical operation of the injector nozzle. This relationship is given in Eq. (I-12), Appendix I.

Plots of the optimum-area pressure ratio versus the injector-to-tunnel stagnation pressure ratio for the test Mach numbers are shown in Fig. 8. In general, the higher the injector-to-tunnel stagnation pressure ratio, the lower the pressure ratio with some exceptions at both ends of the p_{t_j}/p_{t_o} range. At $M_1 = 2.2$ the injector Mach number was never fully established because the pressure ratio required to operate the tunnel at $M_1 = 2.2$ is less than the pressure ratio required for the $M_j = 2.6$ injector.

The approximate maximum p_{t_j}/p_{t_o} at which the tunnel flow could be maintained is shown on the plots by the dashed line labeled "Approximate Maximum p_{t_j}/p_{t_o} for Stability." Injector C would not operate at p_{t_j}/p_{t_o} ratios as high as Injector B possibly because of the greater injection angle which had approximately the same effect as increasing the injector stream static pressure.

The majority of the test was conducted with a tunnel stagnation pressure of 20 psia. With this stagnation pressure, the maximum p_{t_j}/p_{t_o} that could be reached with the available plant capacity was approximately 2.1. Because of this limit there was no experimental verification of the maximum p_{t_j}/p_{t_o} at Mach numbers less than approximately 3.5.

10

The normal shock pressure ratio for the test Mach numbers is shown along the right-hand margin of the plot. The difference between these normal shock pressure ratios and the point where the curves cross the zero p_{t_j}/p_{t_O} axis, or would cross if extrapolated, may be considered as the pressure recovery provided by the geometry of the injector-diffuser configuration without the benefit of the injected air. The indications are that the Injector B geometry, air off, contributes substantially more to the pressure recovery than the Injector A or C geometry. At M = 5.0 the required tunnel pressure ratio for Injector B with the air off was 64 percent of the required pressure ratio for the closed aerodynamic scoop tip. This implies that a worthwhile gain in performance could be achieved by an oversized scoop. Also at M = 5.0 the required tunnel pressure ratio for Injector B with the air on was 48 percent of the required pressure ratio for the aerodynamic tip. Therefore, it appears that injecting air will further reduce the required pressure ratio with a decrement essentially the same as predicted by the simple one-dimensional theory.

A summary of the optimum results obtained with the M_j = 2.6 injectors is presented in Fig. 9. Here the performance of each injector is compared with the normal shock curve (which is used as a reference) and with the closed aerodynamic tip performance (see Fig. 2). Injector B apparently has the best overall performance with an optimum tunnel pressure ratio that is 71 percent of the normal shock value at M_1 = 3.15 and 53 percent of the normal shock pressure ratios for M_1 = 4.0 and 5.0. This corresponds to 60 percent and 48 percent of the pressure ratio required for the closed aerodynamic scoop tip configuration without injection at M_1 = 4.0 and 5.0. The converged-cart configuration provides the lowest pressure ratios between approximately M_1 = 3.35 and M_1 = 5.0 with the largest gain occurring between 3.5 and 4.0. The specific pressure ratio decrements chargeable to this diffuser configuration are 0.18, 0.28, and 0.30 for Mach numbers of 3.5, 4.0, and 5.0, respectively. These general trends indicate the need for an even longer supersonic diffuser at M_1 = 5.0. Injectors A and C show about the same performance in the Mach number range where data are available for both. It was possible at M_1 = 2.2 to lower the pressure ratio to approximately the normal shock value by very careful adjustment of the diffuser using Configuration 4 (see Fig. 6). The setting of this contour was unusually time consuming and therefore could not be used extensively in the test program. A minimum air off point is plotted at M_1 = 5.0 for Injector B and shows, as mentioned previously, that Injector B performs better air off than Injector C with the air on. Testing time limitations did not allow the acquisition of further air off data points.

The influence of injector flow on the starting pressure ratio was only investigated in the model tests at $M_1 = 3.15$ and for the Injector B configuration. The general conclusion reached from these starting data is that the large reduction in the starting pressure ratio found in other injector experiments (that is, Ref. 2) is also present in this arrangement. For the 3.15 Mach number, for example, a 68 percent to 58 percent reduction in the minimum starting pressure ratio over that obtained with a closed aerodynamic tip was indicated with the greater improvement accruing from an injector stagnation pressure ratio near the maximum-running value. These starting pressure ratio points are presented in the following table:

TABLE A
INJECTOR B STARTING PRESSURE RATIO

M_1	M_j	pt_o, psf	θ_j	pt_j/pt_o	λ_s	A_2/A_1
3.15	2.60	2886	0.97	1.978	2.97	0.614
3.15	2.60	2885	0.97	0.983	3.60	0.656

In summary of the model injector results, it should be pointed out that no attempt has been made to optimize the diffuser injector combination and that only a description of the performance of a few system arrangements are presented. There are many parameters that have been more or less glossed over, for example, the optimum injector Mach number and the optimum injection angle, but it has been demonstrated that it is possible to make substantial improvements in the diffuser performance by such a system.

5.0 COMPARISON OF EXPERIMENT AND THEORY

Using the theoretical approach discussed previously and the constants from Table 2, performance characteristics were made for selected values of the variables of interest that correspond to the experimental values. The results are plotted in Figs. 10 and 11.

Figure 10 shows the correlation of the theory and model test data for the average minimum-area static pressure level. The comparison indicates that the hypothetical supersonic diffuser concept (used in the theoretical approach) will provide rough pressure recovery values for a short supersonic diffuser with a centerbody.

12

The usual decrease in pressure ratio as the contraction ratio is decreased, when the other parameters are held constant, is evident in Fig. 11a. The theory does not predict the stable-minimum contraction ratio, so an approximate average of the model test results for this injector tip, discounting slight variations with injector stagnation pressure ratio, is shown as a dotted line in Fig. 11a. This minimum contraction ratio locus, that allows shock-duct stability, was used in subsequent calculations where other parameters are allowed to vary. The pressure ratio so determined is defined as the "Optimum-Area Pressure Ratio, $(\lambda_r)_{opt}$."

The curves in Fig. 11b demonstrate the effect of the injector stagnation pressure, p_{t_j}/p_{t_o}, on the optimum-area pressure ratio. From Eq. (I-12) in Appendix I, it is evident that a variation of this pressure ratio produces a corresponding variation of the mass flow ratio, r, for a fixed-geometry injector, a constant nozzle setting, and constant temperature ratio. For this reason and also to encompass those experiments where the geometry is also variable, the mass flow ratio is sometimes considered the independent variable. By comparison of Figs. 11a and 11b, it may be concluded that the theory predicts that the p_{t_j}/p_{t_o} ratio will have more influence on the optimum tunnel pressure ratio needed to maintain supersonic flow than the diffuser contraction ratio, A_2/A_1. Again, the model results were used to provide a limiting maximum for the stagnation pressure ratio above which a stable shock duct flow field could not be maintained. The stability locus is shown as a dotted line in Fig. 11b.

Also compared in Fig. 11 are the model tunnel results with the theoretical prediction for Injector B. Figure 11a compares the experimental and theoretical effects of diffuser contraction ratio on the minimum running pressure ratio for a constant p_{t_j}/p_{t_o} ratio of approximately 1.5. Here it is seen that the slope of the experimental data is approximately the same as the theory; however, the experimental values are displaced to higher pressure ratios. Figure 11b compares the experimental and theoretical variation of the optimum-area pressure ratio as a function of the injector stagnation pressure ratio, p_{t_j}/p_{t_o}, at the optimum diffuser contraction ratio. Again, the slope of the experimental points is nearly the same as predicted by the theory; however, the values are again displaced to higher pressure ratios.

This disagreement in the level of the experimental and theoretical curves is undoubtedly caused by the deviation of the actual flow field from the simplifying assumptions used in the theoretical analysis. The most notable of these discrepancies is probably the inherent viscous nature of the actual flow field followed by the possibility of incomplete

mixing and severe deviation of the actual flow channel from a simple axisymmetric or a one-dimensional flow field.

Having defined stability limits in terms of both diffuser contraction ratio, A_2/A_1, and injector stagnation pressure ratio, p_{tj}/p_{t_o}, a further application of logic produces some insight into the shock-duct stability problem. Assuming that the expansion or contraction of the injector flow produces an effect on the primary stream similar to a diffuser contraction ratio variation, it is logical to attach significant importance to the static pressure ratio, p_j/p_2. A tolerable maximum in this ratio may be derived from previous theoretical and model test data as follows:

$$(P_j/P_2)_{max} = \frac{(P_{t_j}/P_{t_o})_{max}}{(P_{t_j}/P_j)\,(P_2/P_{t_1})}$$

It may also be reasoned that for small changes in the injector Mach number, while the exit area remains constant, the primary shock-duct stability criteria should be the maximum static pressure ratio, p_j/p_2. Assuming this is the case, an expression for $(p_{tj}/p_{t_o})_{max}$ may be written as follows:

$$(P_{t_j}/P_{t_o})_{max} = (P_j/P_2)_{max} \left(\frac{P_{t_j}}{P_j}\right)\left(\frac{P_2}{P_{t_o}}\right) \tag{5}$$

The effect of varying the injector Mach number on $(p_{tj}/p_{t_o})_{max}$ from Eq. (5) is presented in Fig. 12a. Before this information may be applied to an injector diffuser calculation, however, a law describing the geometric behavior of the injector nozzle as injector Mach number changes must be formulated. Such an expression is as follows:

$$(A/A^*)_j = \frac{125}{216}\,\frac{\left[1 + 0.2M_j^2\right]^3}{M_j} + 0.31167 \tag{6}$$

The first right-hand term in Eq. 6 is, of course, the theoretical relation from Ref. 6. The constant second term in the equation is the added area ratio needed for the M_j = 2.60 Injector B model to account for boundary layer and the type of nozzle construction. Using this equation for the Injector B exit area along with the nozzle sonic area from Table 2, the injector sonic area ratio, A_j^*/A_n^*, was calculated and plotted in Fig. 12b. The decreasing trend in the sonic area ratio with increasing injector Mach number is more than offset by the increasing trend of the stagnation pressure ratio, $(p_{tj}/p_{t_o})_{max}$, so that the mass flow ratio, r, exhibits a net increasing trend shown in Fig. 12c. The optimum pressure ratio for the injector diffuser for these stability assumptions is presented as a function of injector Mach number in Fig. 12d. To take the results illustrated by these figures literally could be misleading for large changes in the injector

14

Mach number from the 2.6 value because the viscous losses will undoubtedly increase slightly with injector Mach number and the process of initially establishing supersonic flow in the injector nozzle itself would become increasingly difficult.

It is believed, however, that a small change in the injector Mach number to 2.8 would result in a net decrease in the optimum pressure ratio, since the viscous and mixing losses should not increase appreciably. The magnitude of this pressure ratio decrement for this small change in the injector Mach number should essentially be that predicted by the simplified theory. From Fig. 11d it is seen that this decrement varies from 0.10 at $M_1 = 3.15$ to 0.42 at $M_1 = 5.0$.

6.0 CONCLUSIONS

From the model tunnel tests of an injector-diffuser and the simplified theoretical analysis, the following conclusions may be formulated:

1. Based on the model test results, Injector B gave performance superior to Injectors A and C, both of which performed about equally.

2. At M = 5.0, the required tunnel pressure ratio for Injector B with the air off was 64 percent and with the air on was 48 percent of the required pressure ratio for the closed aerodynamic scoop tip.

3. The best injector configuration, Injector B, operating near the maximum stable injector stagnation pressure ratio, $(P_{t_j}/P_{t_o})_{max}$, and optimum diffuser geometry produced an optimum pressure ratio required to maintain supersonic flow that was 71, 53, and 53 percent of the normal shock value for Mach numbers of 3.15, 4.00, and 5.00, respectively.

4. At $M_1 = 3.5$ and above, operation with the rear split cart as a diffuser element produced an optimum pressure ratio decrement of 0.18, 0.28, and 0.30 for Mach numbers of 3.50, 4.00, and 5.00, respectively.

5. From the limited amount of experimental starting pressure ratio data that was obtained for Injector B at a test section Mach number of 3.15, it may be concluded that the large reduction in the starting pressure ratio requirements found in other injector experiments is also present in this arrangement.

6. The simple one-dimensional theory and the model test results indicate that the influence of the p_{t_j}/p_{t_o} ratio is more pronounced on the minimum tunnel pressure ratio required to maintain supersonic flow than the contraction ratio.

7. The simple one-dimensional theory can indicate the effect of varying geometric and flow parameters. However, the theory cannot accurately predict the overall injector-diffuser pressure recovery.

8. Increasing the injector Mach number M_j slightly above 2.6 to 2.8 should allow stable operation at larger injector stagnation pressure ratios, $(p_{t_j}/p_{t_o})_{max}$, which would result in a reduction of the optimum pressure ratio by a decrement of approximately 0.1 at $M_1 = 3.15$ to 0.42 at $M_1 = 5.0$.

REFERENCES

1. Spiegel, J. M., Hofstetter, R. V. and Kuehn, D. M. "Applications of Auxiliary Air Injectors to Supersonic Wind Tunnels." NACA RM A53I01, November 1953.

2. Hunczak, H. R. and Rousso, M. D. "Starting and Operating Limits of Two Supersonic Wind Tunnels Utilizing Auxiliary Air Injection Downstream of the Test Section." NACA TN3262, September 1954.

3. Carter, E. C. and Tucker, K. F. "Some Results of an Investigation into the Use of Air Injection in a Model of the Diffuser for the A. R. A. Supersonic Tunnel." Aeronautical Research Council, (Grt. Brit.) A. R. A. Report No. 1, C. P. No. 386, August 1957.

4. Hasel, L. E. and Sinclair, A. R. "A Preliminary Investigation of Methods for Improving the Pressure-Recovery Characteristics of Variable-Geometry Supersonic-Subsonic Diffuser Systems." NACA RM L 57 H02, October 1957.

5. Foa, J. V. "Mach Number Functions for Ideal Diatomic Gases." Cornell Aeronautical Laboratory, Inc., (A. T. I. 104160), October 1949.

6. Ames Research Staff. "Equations, Tables and Charts for Compressible Flow." NACA Report 1135, 1953.

7. Parkhurst, R. C. and Holder, D. W. Wind Tunnel Technique. Pitman Publishing Corporation, London, 1952. (p. 52)

8. Evvard, J. C. and DeMarquis, D. W. "Investigation of a Variable Mach Number Supersonic Tunnel with Non-Intersecting Characteristics." NACA RM E8J13, November 1948.

9. McLafferty, George. "A Generalized Approach to the Definition of Average Flow Qualities in Non-Uniform Streams." United Aircraft Corporation, SR-13534-9, December 1955.

10. Kennedy, E. C., Sonheim, D. W. and Barnes, A. M. "New Mach Tables for Ram-Jet Flow Analysis." Ordnance Aerophysics Laboratory, OAL Memorandum 50, August 1956.

11. Riise, H. N. "Compressible Flow Tables for Air in Increments of 0.001 in Mach Numbers." Jet Propulsion Laboratory, California Institute of Technology, Publication No. 27, August 1954.

APPENDIX 1

DERIVATION OF EQUATIONS FOR THE SIMPLIFIED
INJECTOR-DIFFUSER THEORY

For a selected supersonic diffuser configuration, providing the length of the diffuser does not require the accounting for reflected waves, the following relations may be assumed to be applicable:

$$\frac{P_2}{P_{t_1}} = \frac{7M_1^2 \sin^2 \theta_e - 1}{6} \left[\frac{5}{M_1^2 + 5} \right]^{7/2} \tag{I-1}$$

and

$$\tan \delta_e = \frac{5 \cot \theta_e \ (M_1^2 \sin^2 \theta_e - 1)}{5 + M_1^2 \ (6 - 5 \sin^2 \theta_e)} \tag{I-2}$$

These equations, of course, are the familiar two-dimensional oblique shock relations relating the flow deflection and shock wave angles and the static pressure behind an oblique shock to the test section stagnation pressure (from Ref. 6). The definition of the effective flow deflection angle is formulated by an assumed relation whereby both the centerbody and sidewall area changes are reduced to an equivalent wedge angle based on the length of the first diffuser leaf. Mathematically:

$$\sin \delta_e = \frac{A_1 \ (1 - A_2/A_1)}{h \ (\Delta L_1)} \tag{I-3}$$

where

h = Tunnel height, in.

ΔL_1 = First diffuser leaf length, in.

A_2/A_1 = Diffuser contraction ratio accounting for the centerbody area.

Now for mass flow continuity:

$$m_n^* = m_2 \quad \text{or} \quad W_n^* = W_2 \tag{I-4}$$

The definition of the static pressure mass flow function, $\overset{\circ}{m}$, (Refs. 9 and 10):

$$\overset{\circ}{m} = \frac{W \sqrt{T_t}}{p A} = 0.91891 \ M \left[1 + 0.2M^2 \right]^{1/2} \tag{I-5}$$

combined with Eq. (I-4) yields the mass flow function at Station 2, $\overset{\circ}{m}_2$, which may be expressed in the form:

$$\overset{\circ}{m}_2 = \frac{0.53177}{\left(\dfrac{P_2}{P_{t_1}} \right) \ \left(\dfrac{A_1}{A_n^*} \right) \left(\dfrac{A_2}{A_1} \right)} \tag{I-6}$$

Where the area ratio, A_1/A_n^*, is defined as a function of M_1 from isentropic flow tables (see Ref. 11); the diffuser contraction ratio, A_2/A_1, is a function of the diffuser geometry, and the pressure ratio, p_2/p_{t_1}, is given by Eq. (I-1).

The mass flow function, $\overset{\circ}{m}_2$, defined by Eq. (I-6) may now be used to define the Mach number, M_2, from the tables in Ref. 10, or using Eq. (I-5) may be explicitly expressed as:

$$M_2 = \left[-2.50 + \sqrt{6.250 + 5.9214\ \overset{\circ}{m}_2{}^2}\right]^{1/2} \tag{I-7}$$

Now the equations to describe the energy addition and subsequent diffusion in an injector diffuser process may be developed using the following assumptions:

1. The flow field is one-dimensional.
2. Viscous losses are neglected.
3. Mixing is complete.
4. The mixing process takes place in a constant area channel.
5. The shock losses in the constant area channel are equivalent to a single normal shock at the end of the mixing length.
6. The subsonic diffuser losses may be expressed in terms of a constant diffuser efficiency.

The resulting flow model is shown schematically in the following sketch:
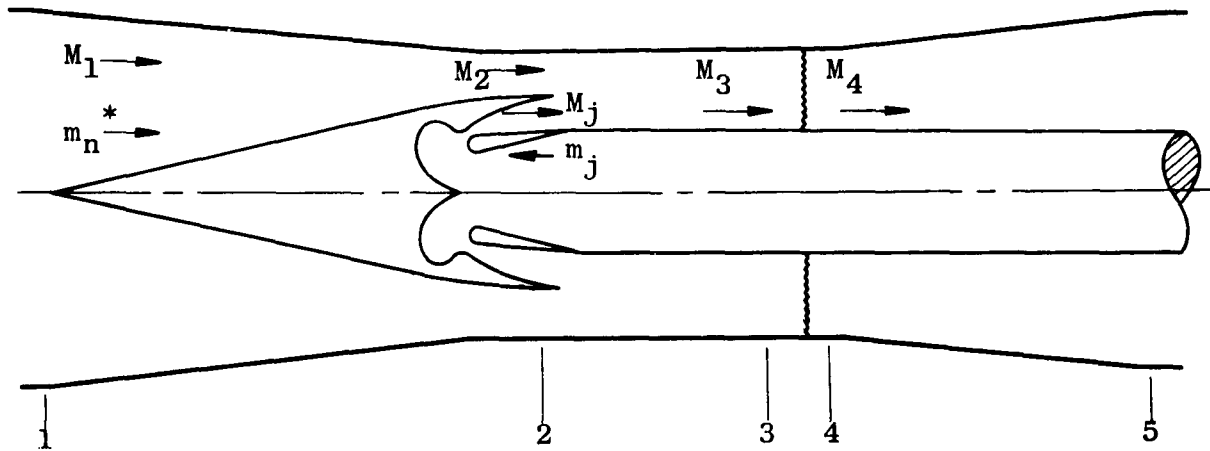
To simplify the formulation of the equations, the following Mach number functions using $\gamma = 7/5$ (see Ref. 2 or 5) are defined:

$$D = \frac{M}{\left(1 + 0.2M^2\right)^3} \tag{I-8}$$

$$G = \frac{1 + 1.4M^2}{\left(1 + 0.2M^2\right)^{7/2}} \tag{I-9}$$

$$N = \frac{M\left(1 + 0.2M^2\right)^{1/2}}{1 + 1.4M^2} \tag{I-10}$$

Using these functions and the simplifying assumptions previously stated, the flow process between Stations 1, 2, and 3 may be written in terms of the stagnation conditions as follows (from Ref. 2):

Continuity:

$$m_2 + m_j = m_3$$

$$\frac{P_{t_1} A_1 D_1}{\sqrt{T_{t_1}}} = \frac{P_{t_2} A_2 D_2}{\sqrt{T_{t_2}}} = \frac{P_{t_j} A_j D_j}{r\sqrt{T_{t_j}}} = \frac{P_{t_3} A_3 D_3}{(1+r)\sqrt{T_{t_3}}} \tag{I-11}$$

where

$$r = \frac{m_j}{m_2} = \frac{m_j}{m_n^*} = \left(\frac{P_{t_j}}{P_{t_1}}\right)\left(\frac{A_j^*}{A_n^*}\right)\frac{1}{\sqrt{\theta_j}} \tag{I-12}$$

and

$$\theta_j = \frac{T_{t_j}}{T_{t_1}}$$

Momentum:

$$P_{t_2} A_2 G_2 + P_{t_j} A_j G_j = P_{t_3} A_3 G_3 \tag{I-13}$$

when

$$A_2 + A_j = A_3$$

Energy:

$$m_2 c_p T_{t_2} + m_j c_p T_{t_j} = m_3 c_p T_{t_3} \tag{I-14}$$

which reduces to the form:

$$\frac{T_{t_3}}{T_{t_2}} = \frac{1 + r\theta_j}{1 + r} = \frac{T_{t_3}}{T_{t_1}} \quad \left(\text{Adiabatic flow,} \quad T_{t_2} = T_{t_1}\right) \tag{I-15}$$

Combining Eqs. (I-11), (I-13), and (I-14)

$$N_3 = \frac{(1 + r)^{1/2} (1 + r\theta_j)^{1/2}}{\dfrac{1}{N_2} + \dfrac{r\theta_j^{1/2}}{N_j}} \tag{I-16}$$

which for $\theta_j = 1$ reduces to the form:

$$N_3 = \frac{1 + r}{\dfrac{1}{N_2} + \dfrac{r}{N_j}} \tag{I-17}$$

21

Equations (I-16) and (I-17) are implicit functions of M_3 which are conveniently solved for M_3 by the tables in Ref. 5; however, two solutions can be obtained: (1) a subsonic M_3 and (2) a supersonic M_3. The subsonic solution is disregarded for those cases of clear-cut supersonic mixing as considered in this report.

Now since,

$$\frac{A_2}{A_n{}^*} = \left(\frac{A_2}{A_1}\right)\left(\frac{A_1}{A_n{}^*}\right) \tag{I-18}$$

Equations (I-13) and (I-18) may be combined and arranged to obtain:

$$\frac{P_{t_3}}{P_{t_1}} = \frac{P_{t_2}}{P_{t_1}}\left[\frac{\left(\frac{A_2}{A_1}\right)\left(\frac{A_1}{A_n{}^*}\right)}{\left(\frac{A_2}{A_1}\right)\left(\frac{A_1}{A_n{}^*}\right) + \frac{A_j}{A_n{}^*}}\right]\frac{G_2}{G_3} + \frac{P_{t_j}}{P_{t_1}}\left[\frac{\dfrac{A_j}{A_n{}^*}}{\left(\frac{A_2}{A_1}\right)\left(\frac{A_1}{A_n{}^*}\right) + \frac{A_j}{A_n{}^*}}\right]\frac{G_j}{G_3} \tag{I-19}$$

Equation (I-19) may be conveniently thought of as the weighted addition of the stagnation pressure ratios of the two streams with geometry-momentum scaling coefficients.

The supersonic diffuser total pressure ratio, p_{t2}/p_{t1}, may be obtained from isentropic functions (see Ref. 6):

$$\frac{P_{t_2}}{P_{t_1}} = \frac{P_2}{P_{t_1}}\left[1 + 0.2M_2{}^2\right]^{7/2} \tag{I-20}$$

where p_2/p_{t1} and M_2 are obtained from Eqs. (I-1) and (I-7), respectively.

TABLE 1

PWT-SMT INJECTOR NOZZLE CONTOUR ORDINATES, $M_i \cong 2.6$

X, in.	Y, in.	X, in.	Y, in.
0	0.94395	1.79948	0.52342
0.24030	0.94238	2.05028	0.39142
0.38160	0.93660	2.32328	0.23108
0.52035	0.92468	2.62028	0.03772
0.66525	0.90540	2.94345	−0.19372
0.81915	0.87682	3.29528	−0.46740
0.98452	0.83738		
1.16385	0.78495		
1.35802	0.71685		
1.56938	0.63068		
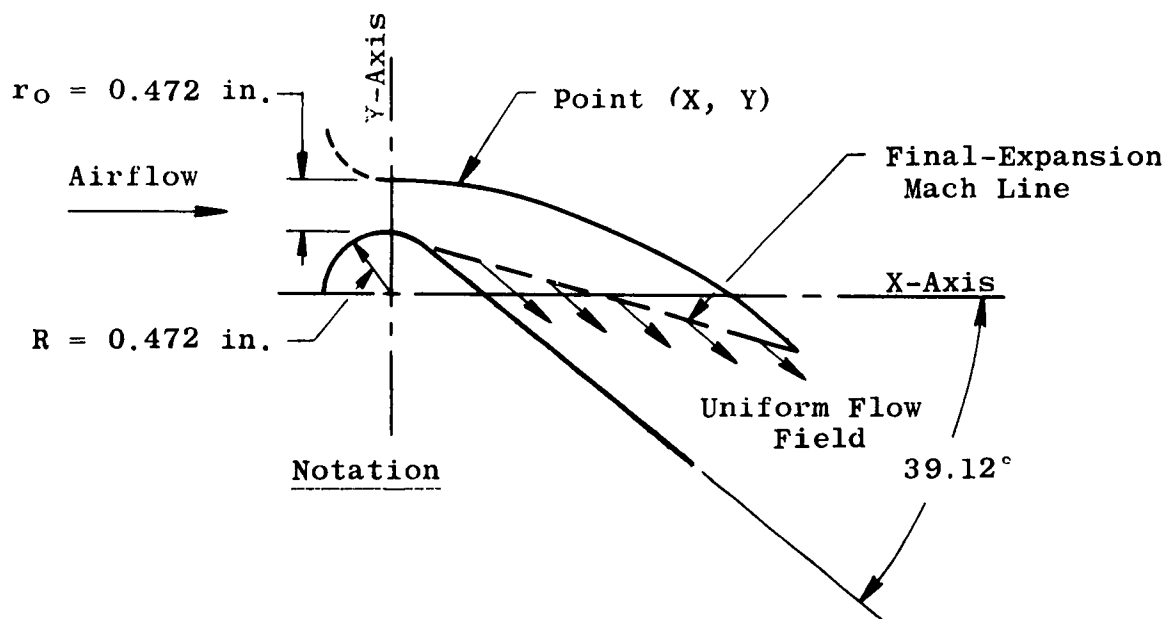
TABLE 2

GEOMETRIC CONSTANTS FOR A CENTERBODY INJECTOR-DIFFUSER,
SUPERSONIC MODEL TUNNEL, $M_i \cong 2.6$

Nozzle Contour M_1	A_n^*, $in.^2$	A_1/A_n^*	A_j/A_n^* (Inj. A, B, & C)	A_j^*/A_n^* (Inj. A & B)	A_j^*/A_n^* (Inj. C)
1.60	112.008	1.250	0.28707	0.08661	0.08449
2.20	69.024	2.005	0.46633	0.14069	0.13725
3.15	27.000	4.884	1.19216	0.35968	0.35088
3.50	18.744	6.790	1.71734	0.51813	0.50545
4.00	12.804	10.720	2.51411	0.75851	0.73996
5.00	4.860	25.000	6.62311	1.99822	1.94933
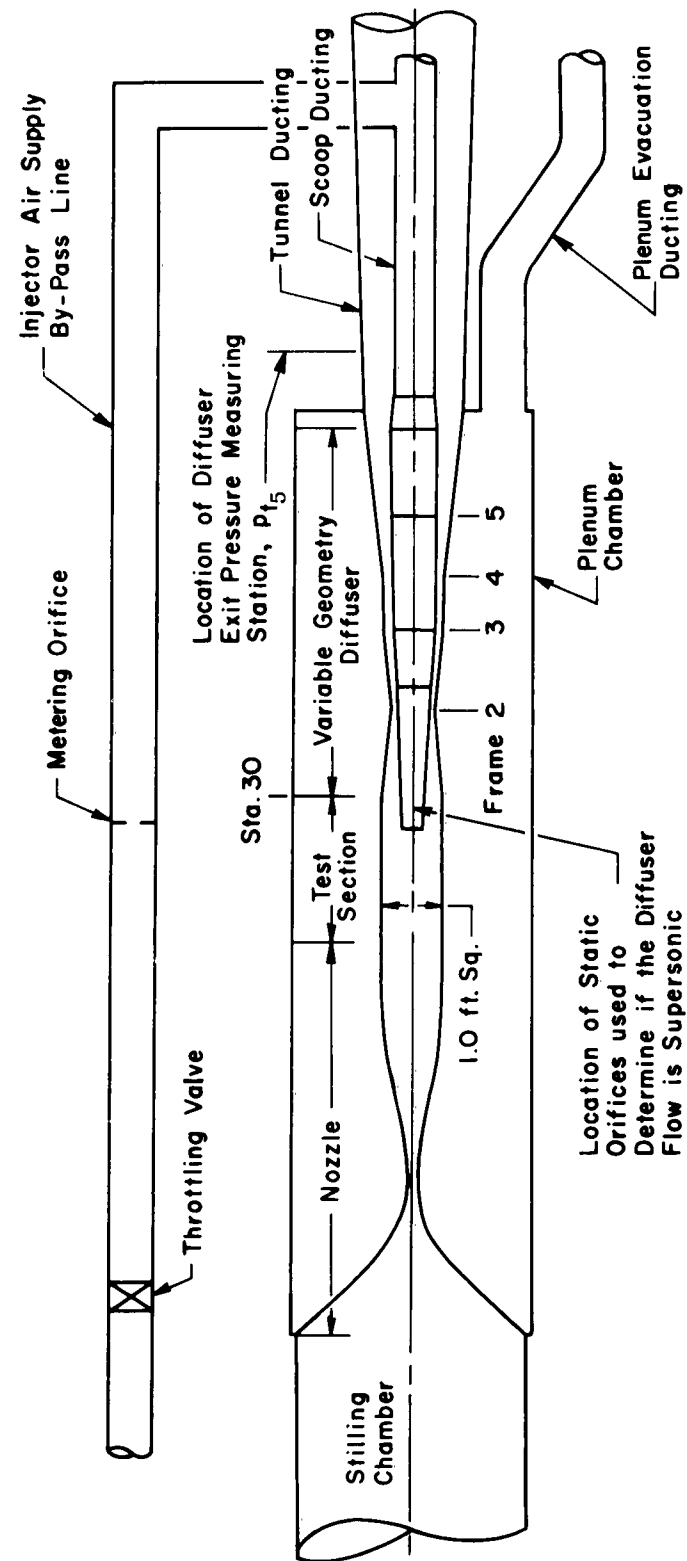
Fig. 1 Schematic of the Supersonic Model Tunnel

Tangent to the Scoop
Duct at this Point

Sta 51.9

R = 106.61 in.

Sta 30
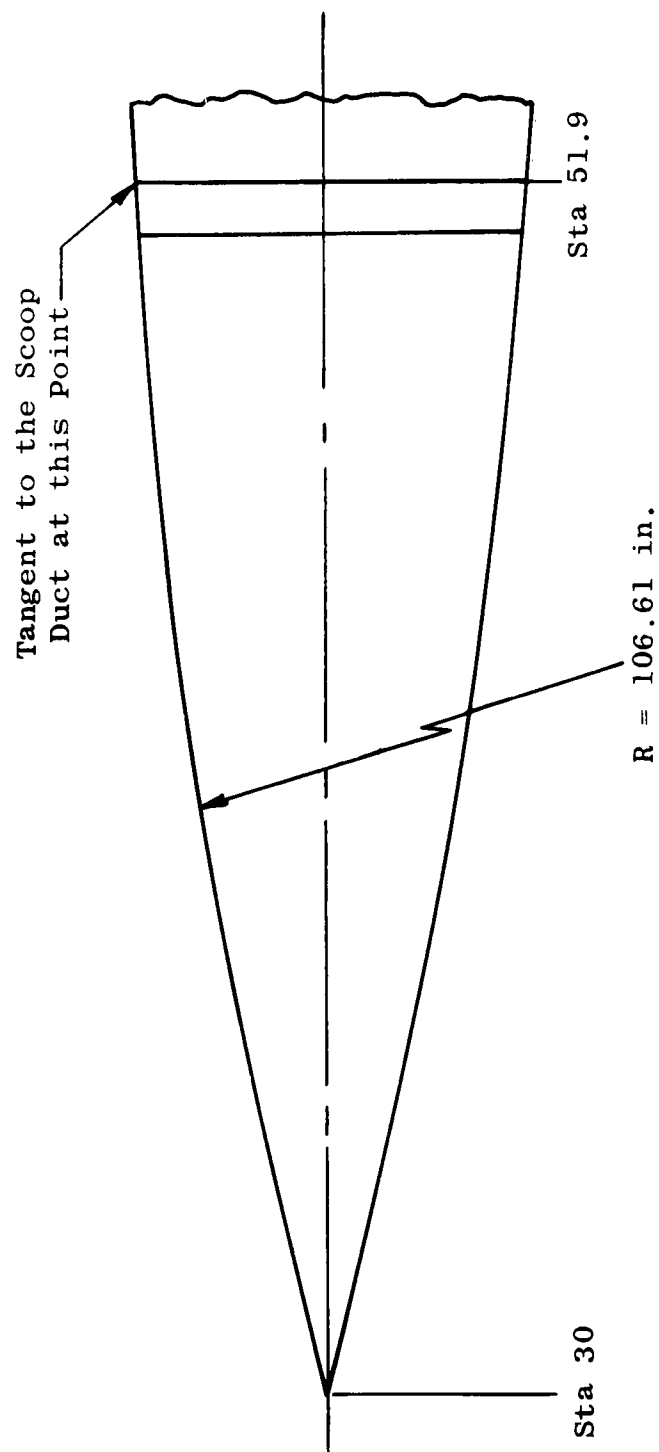
Fig. 2 Closed Aerodynamic Scoop Tip

Notes:

1. The Quarter-Section Construction
   Details are Representative of the
   Model

2. The Fore-Tip is Supported at the
   Downstream end by Eight
   Radial Divider Plates Approx-
   imately 1/16 Inch Thick

11°

Wedge Fore-Tip

Sta. 31.90
Outside Dia.

38.42

45.05
7.125

49.50   51.21
9.488   9.675

PLAN VIEW

Location of 4 Static Orifices p_j

Location of 4 Static Orifices —
p_{2v} and p_{2h}

0.50 Inch (Typ.)

Total Pressure Tube, p_{tj}

m_j

Cusp

3.05° Flow Injection
Angle

Support Strut

0   2   4   6

Scale-Inch

SIDE VIEW
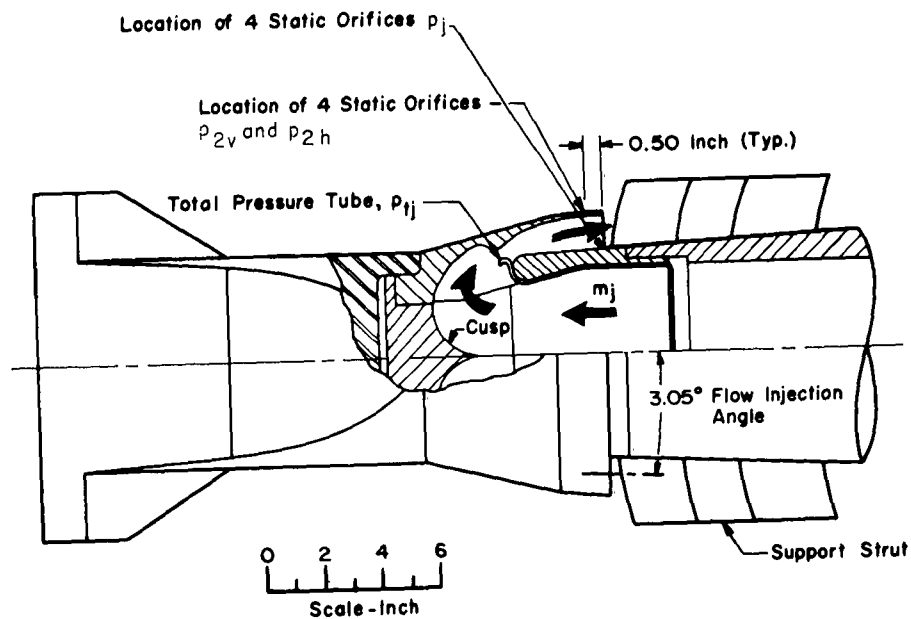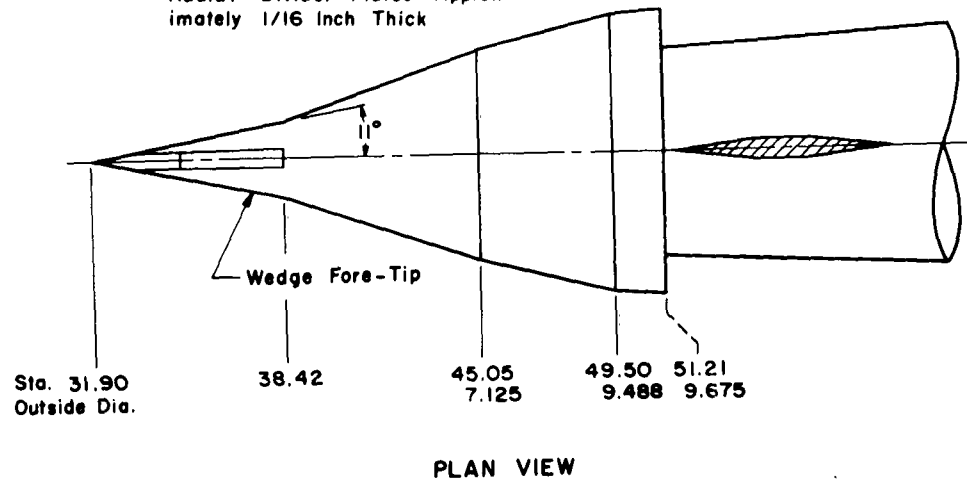
Fig. 3 Injector A Geometry, $A_i^* = 9.71$ in.^{2}, $A_i = 32.19$ in.^{2}, and $M_i \cong 2.6$

Notes:

1. The Quarter-Section Construction Details are Representative of the Model

2. The Fore-Tip is Supported at the Downstream end by Eight Radial Divider Plates Approximately 1/16 Inch Thick

Location of Static Orifices, p_j

Location of Static Orifices p_{2v} and p_{2h}

Total Pressure Tube, p_{tj}

Conic Frustum Fore-Tip

0 2 4 6
Scale-Inch

0.50 Inch (Typ.)

m_j

Cusp

3.05° Flow Injection Angle

Support Strut

Sta.	18.825	24.412	31.912	38.625	45.052	51.210
Outside Dia.	2.992	5.835	7.800	9.000	9.675	

Fig. 4 Injector B Geometry, $A_i^* = 9.71$ in.^{2}, $A_i = 32.19$ in.^{2}, and $M_i \cong 2.6$

Notes:

1. The Quarter-Section Construction Details are Representative of the Model

2. The Fore-Tip is Supported at the Downstream end by Eight Radial Divider Plates Approximately 1/16 Inch Thick

Location of Static Orifices, p_j

Location of Static Orifices, p_{2v} and p_{2h}

Total Pressure Tube, p_{tj}

Conic Frustum Fore-Tip

0 2 4 6
Scale-Inch

0.50 Inch (Typ.)

m_j

Cusp

15° Flow Injection Angle

Support Strut

Sta.	26.325	31.912	39.412	43.380	46.965	49.185
Outside Dia.	2.992	5.835	6.998	7.500	7.500	

Fig. 5 Injector C Geometry, $A_i^* = 9.48$ in.^{2} and $M_i \cong 2.6$

28
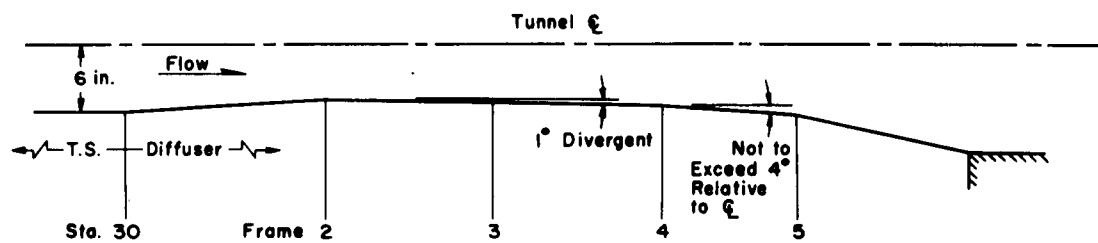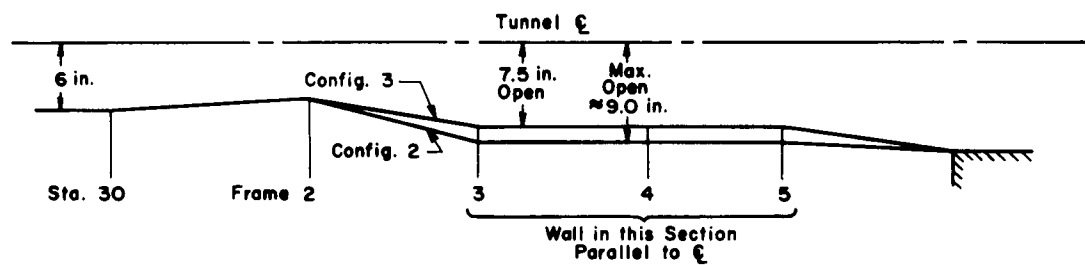
a. Configuration 1

b. Configurations 2 and 3
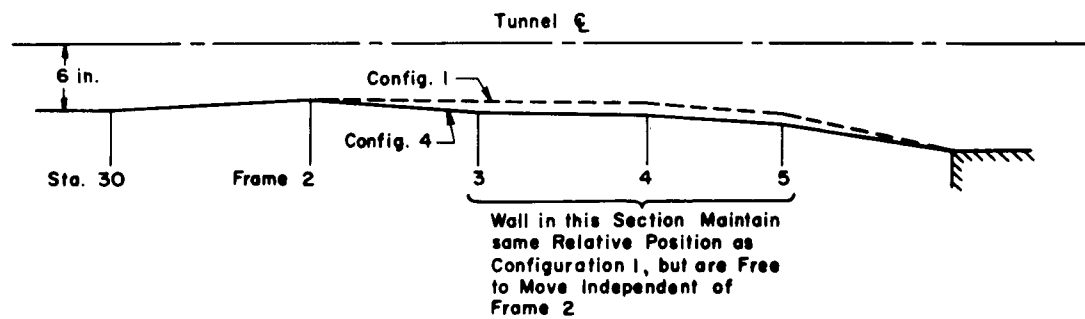
c. Configuration 4

Note: Minimum Area Occurs at
Frame 2 for all Configurations

Fig. 6 Variable Geometry Diffuser Contours Used in the Model Tunnel Injector Tests

29

a. Injector B, Diffuser Contour Configuration 1

b. Injector C, Diffuser Contour Configuration 4
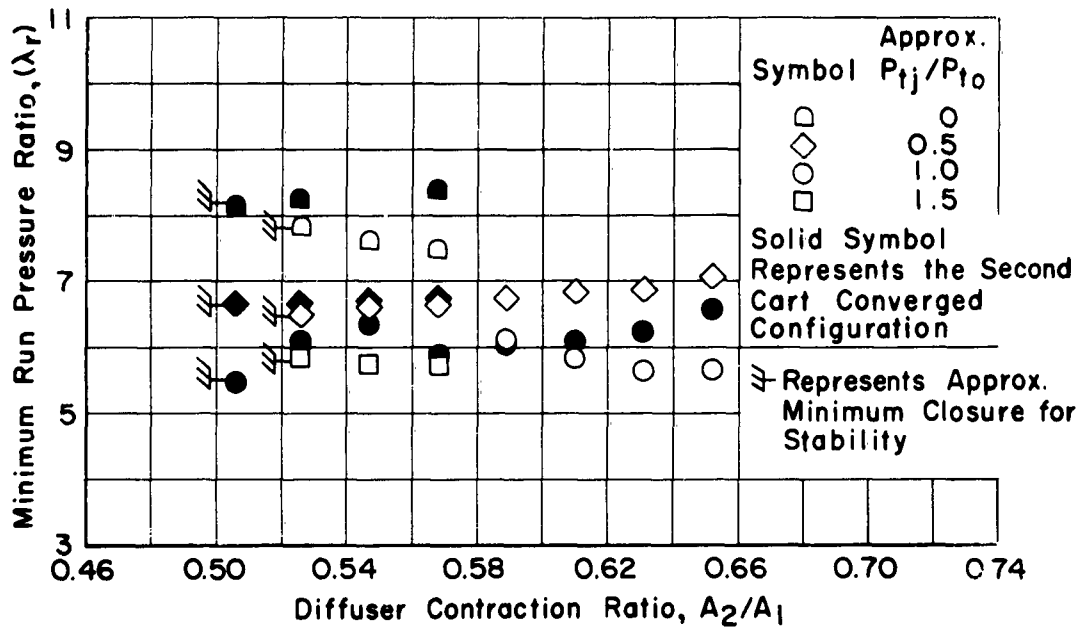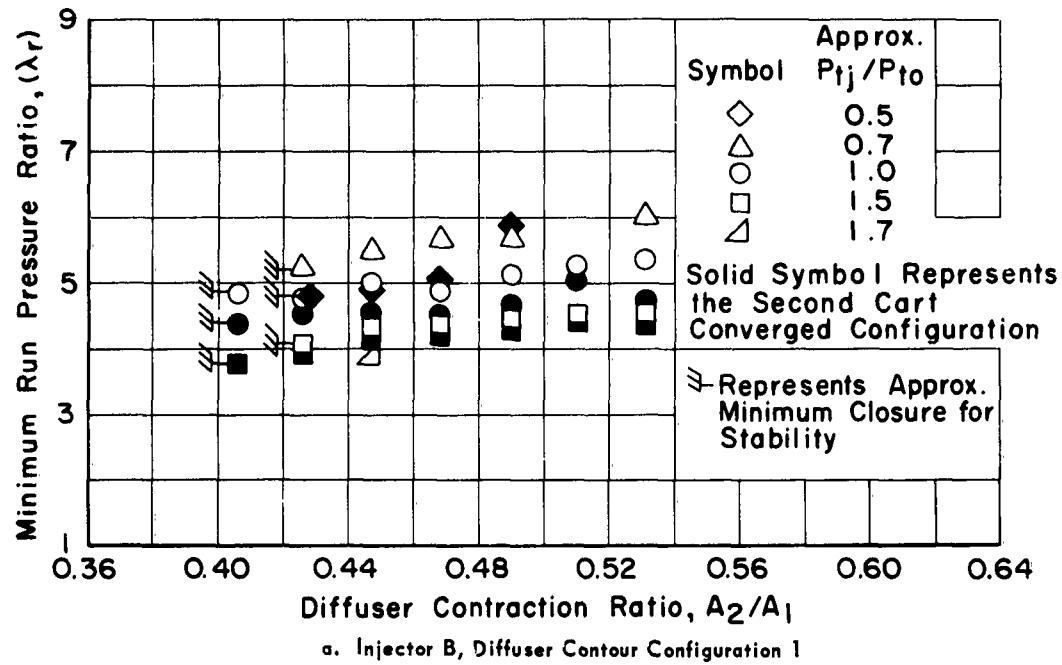
Fig. 7 Typical Model Injector-Diffuser Performance, $M_1 \cong 4.00$, $M_j \cong 2.60$, $p_{t_o} \cong 2880$ psf, and $T_{t_o} \cong 100°F$

30
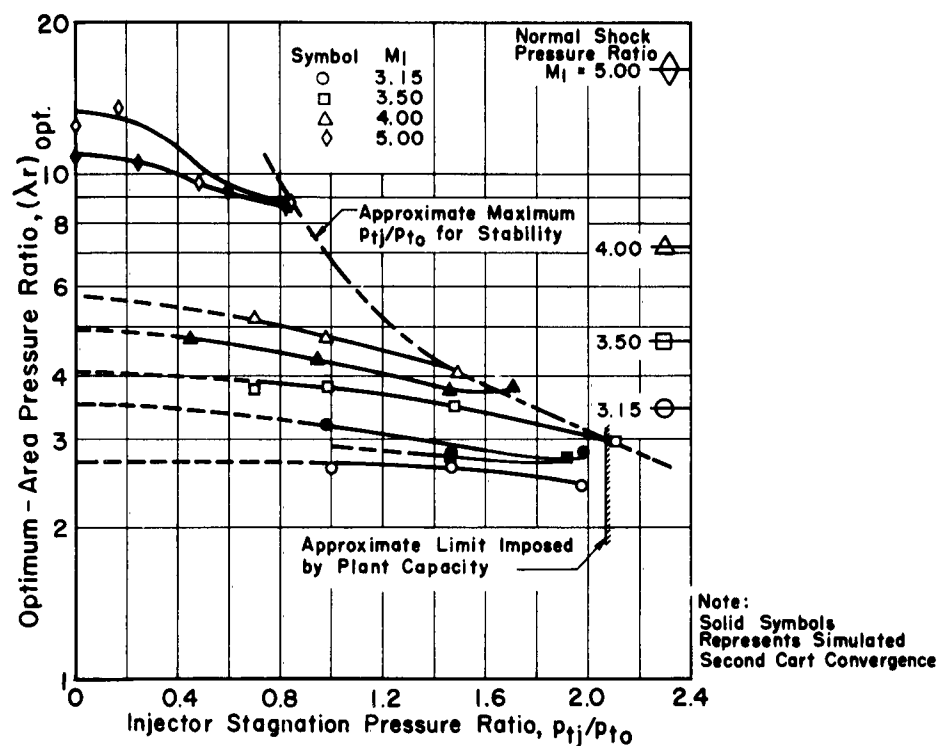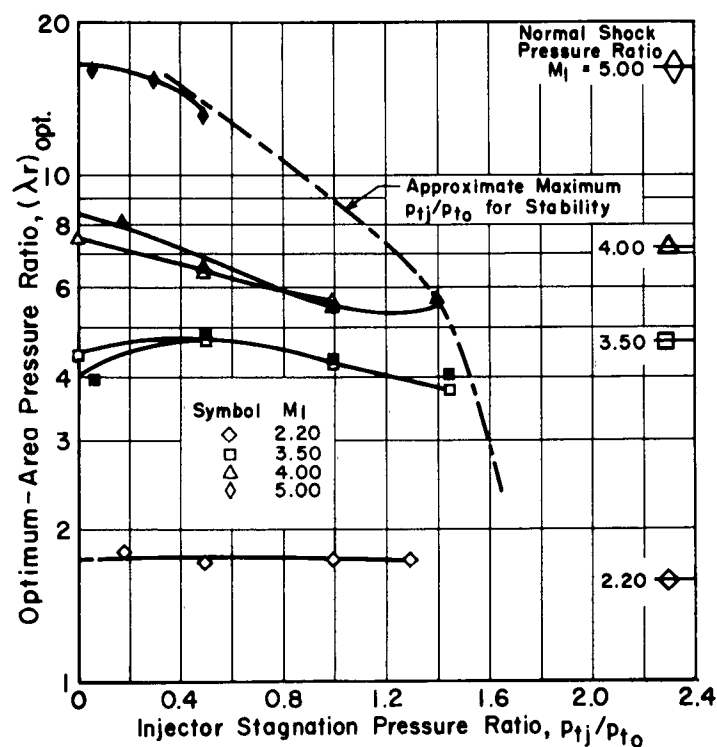
a. Injector B

b. Injector C

Fig. 8 Injector-Diffuser Performance as a Function of the Injector Stagnation Pressure Ratio, $A_2/A_1 \cong$ Stable Minimum, $M_i \cong 2.6$, and $\theta_i \cong 1.0$

31

Sym	Injector	p_{t_o} PSF	T_{t_o} °F	p_{t_j}/p_{t_o}	θ_j	A_2/A_1
▫	A	1324	106	1.414	0.950	0.739
◌	A	1654	100	1.116	0.960	0.718
◇	A	2928	103	0.644	0.960	0.697
■	B	2851	98	1.477	0.993	0.572
□		2855	105	2.032	0.998	0.468
●	B	2904	106	1.924	0.998	0.406
○		2876	96	2.119	0.998	0.426
▲	B	2932	99	1.469	0.996	0.406
△		2865	104	1.489	0.998	0.426
◆	B	4879	107	0.828	0.97±0.020	0.385
◇		4935	140	0.847	0.97±0.020	0.406
◣	B	4872	109	Injector-Off		0.364
◿ₓ	C	2885	110	Injector-Off		0.735
◖ₓ	C	2887	103	Injector-Off		0.589
▲ₓ	C	2896	123	0.990	1.000	0.506
◆ₓ	C	5793	154	0.502	1.000	0.547

Solid Symbol Represents Simulated Second
Cart Convergence
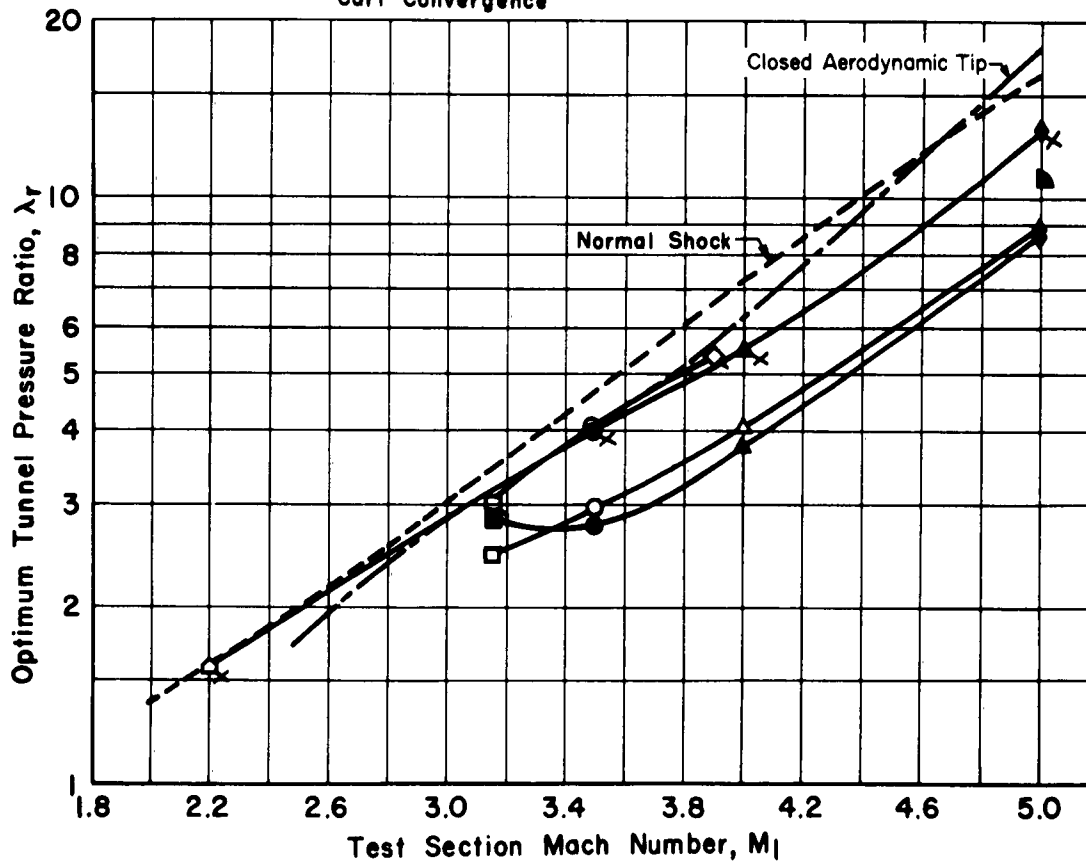
Fig. 9 Summary of Optimum Empty-Tunnel Diffuser Performance, $M_j \cong 2.6$,
$A_2/A_1 \cong$ Stable Minimum, $p_{t_o} \cong 2880$ psf, and $T_{t_o} \cong 100°$F

32

a. Injector B
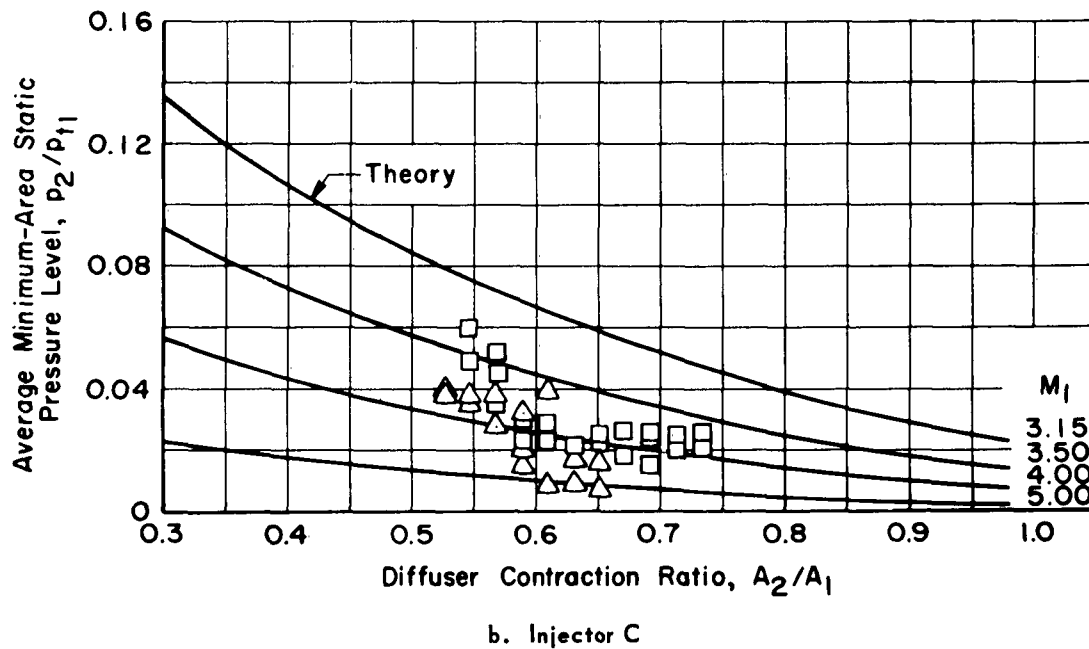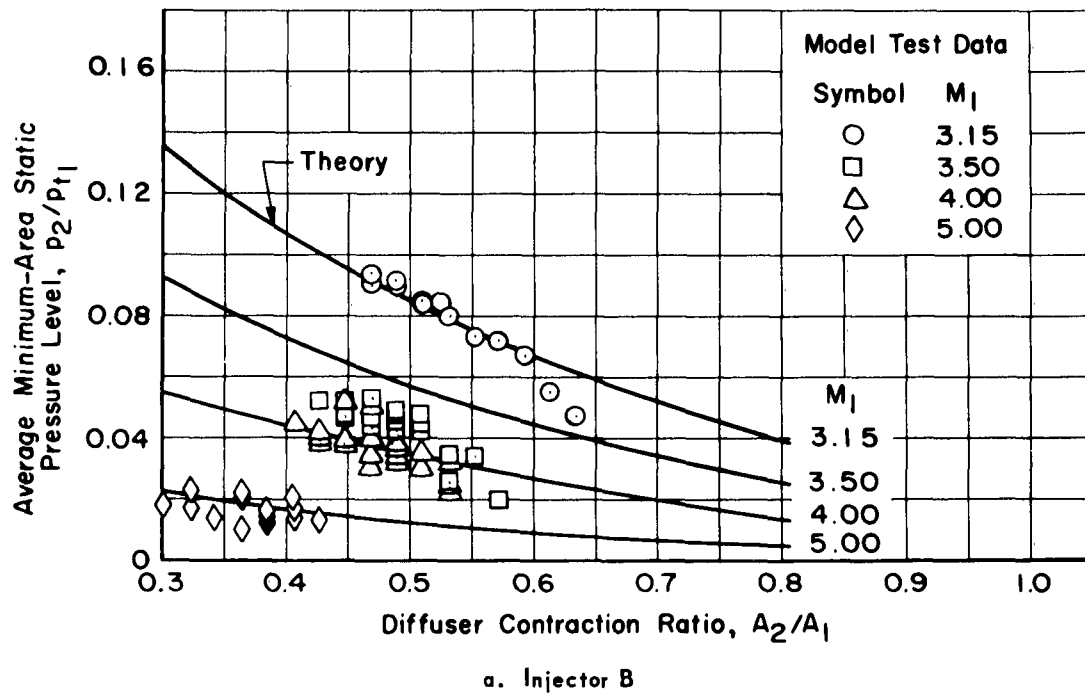
b. Injector C

Fig. 10 Correlation of Theory (Eq. 1 – 1) and Model Test Data for the Average Minimum-Area Static Pressure Level
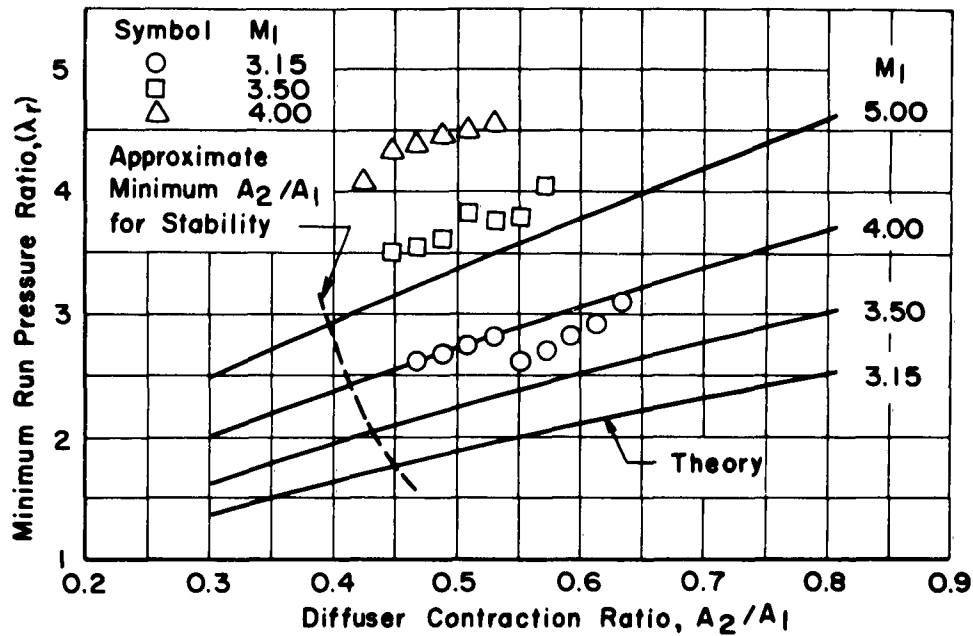
a. Diffuser Contraction Ratio Variation, $p_{t_i}/p_{t_o} \cong 1.5$
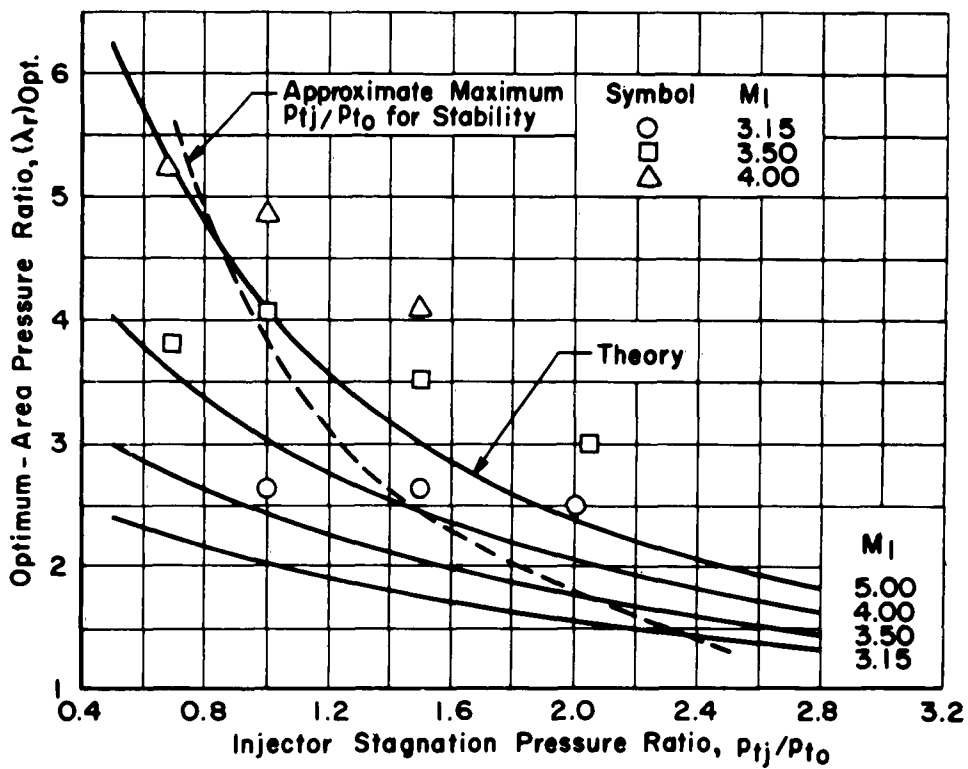
b. Injector Stagnation Pressure Ratio Variation, $A_2/A_1 \cong$ Stable Minimum

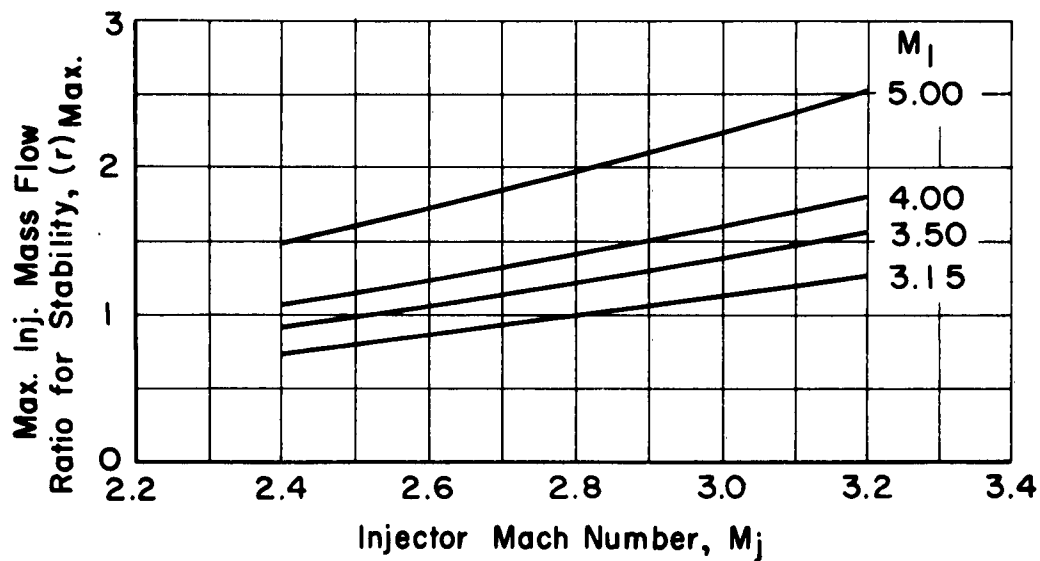Fig. 11 Comparison of Theory and Experiment, Injector B, $M_i \cong 2.60$ and $\theta_i \cong 1.0$

34
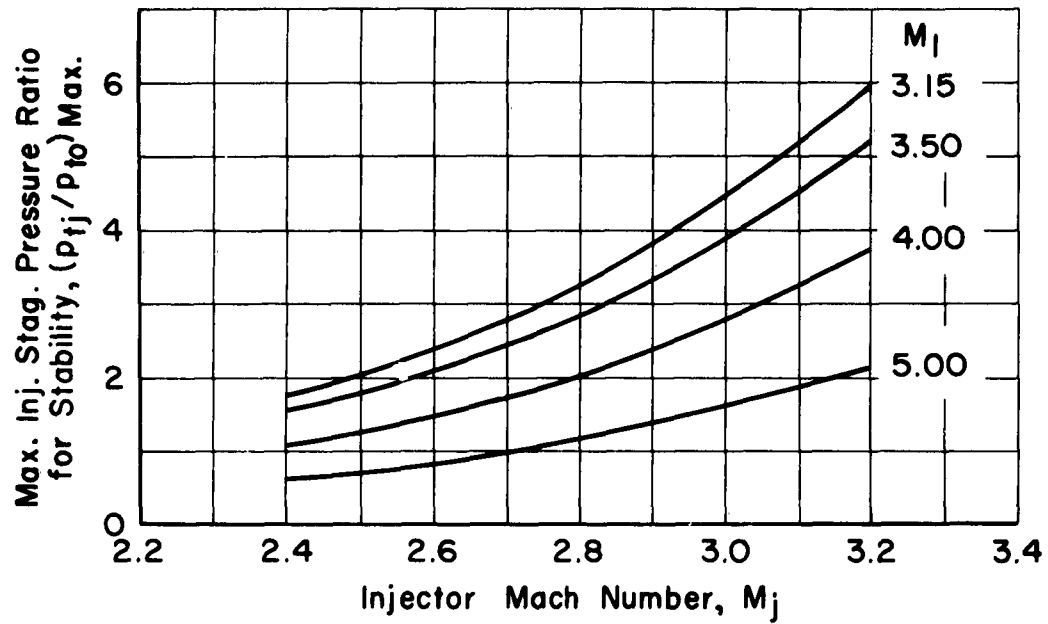
a. Maximum Injector Stagnation Pressure Ratio for Stability, A_2/A_1 = Stable Minimum and p_i/p_2 = Stable Maximum
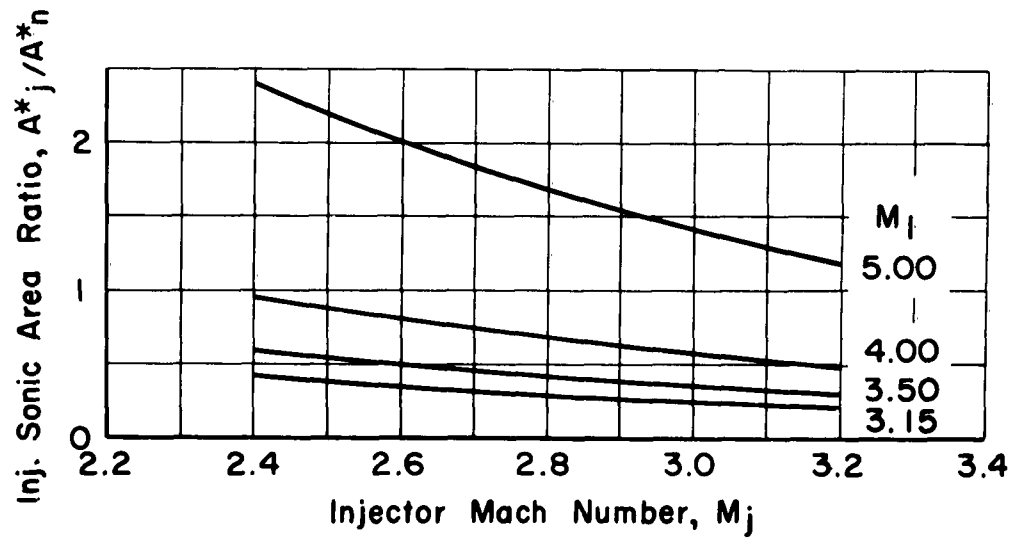
b. Injector Sonic Area Ratio

Fig. 12 Effect of Varying the Injector Mach Number on Various Injector B Parameters from Simplified Theory, A_i = 32.19 in.^{2}, p_i/p_2 = Stable Maximum, and θ_i = 1.0

35

c. Maximum Injector Mass Flow Ratio for Stability, A_2/A_1 = Stable Minimum, P_{t_j}/P_{t_o} = Stable Maximum, and θ_j = 1.0

d. Optimum-Area Pressure Ratio, A_2/A_1 = Stable Minimum, P_{t_j}/P_{t_o} = Stable Maximum, and θ_j = 1.0

Fig. 12 Concluded

Arnold Engineering Development Center
Arnold Air Force Station, Tennessee
Rpt. No. AEDC-TDR-62-75. FEASIBILITY OF A DIF-
FUSER CENTERBODY INJECTOR FOR THE 16-FOOT
SUPERSONIC TUNNEL OF THE PROPULSION WIND
TUNNEL FACILITY. April 1962, 44 p. incl 11 refs.,
illus., tables.   Unclassified Report

A centerbody injector for reducing the pressure ratio re-
quired to operate the 16-Ft Supersonic Tunnel of the
Propulsion Wind Tunnel Facility has been investigated
analytically, and several configurations have been tested
in the Supersonic Model Tunnel. The injectors were
fitted to the existing scavenging scoop centerbody so that
secondary air routed through the scavenge ducting is in-
troduced just downstream of the minimum area of the

variable geometry diffuser. The results obtained from
the best tip injector system, with respect to the running
pressure ratio at M = 5.0, ranged from a 36-percent
improvement with the injector air off to a 52-percent
improvement with the maximum tolerable air injection
over the data from the closed aerodynamic scoop tip.

1. Injectors
2. Supersonic wind tunnels
3. Supersonic diffusers
4. Pressure
5. Tests
6. Analysis
I. AFSC Program Area 750A,
   Project 8950, Task 895001
II. Contract AF 40(600)-800
    S/A 24(61-73)
III. ARO, Inc., Arnold AF Sta.,
     Tenn.
IV. E. H. Sloan, Jr. and
    M. W. Davis
V. Available from OTS
VI. In ASTIA collection